Marine Pollution Bulletin 184 (2022) 114109

Contents lists available at ScienceDirect

Marine Pollution Bulletin

journal homepage: www.elsevier.com/locate/marpolbul

Peculiar polycyclic aromatic hydrocarbons accumulation patterns in a non-zooxanthellate scleractinian coral

Frapiccini Emanuela [a,d,1], Caroselli Erik [b,d,1], Franzellitti Silvia [c,d], Prada Fiorella [a,d,2], Marini Mauro [a,d,*], Goffredo Stefano [a,d]

[a] Institute of Biological Resources and Marine Biotechnology (IRBIM), National Research Council (CNR), Largo Fiera della Pesca 2, 60125 Ancona, Italy
[b] Marine Science Group, Department of Biological, Geological and Environmental Sciences, University of Bologna, via Selmi 3, 40126 Bologna, Italy
[c] Animal and Environmental Physiology Laboratory, Department of Biological, Geological and Environmental Sciences, University of Bologna, via S. Alberto 163, 48123 Ravenna, Italy
[d] Fano Marine Center, The Inter-Institute Center for Research on Marine Biodiversity, Resources and Biotechnologies, Viale Adriatico 1/N, 61032 Fano, Italy

ARTICLE INFO

Keywords:
Bioaccumulation
Leptopsammia pruvoti
Mediterranean Sea
PAH
QuEChERS
Trophic strategy

ABSTRACT

Assessing the sources and accumulation patterns of polycyclic aromatic hydrocarbons (PAHs) in corals is critical, as they threaten coral ecosystem resilience in addition to other anthropogenic pressures. We determined acenaphthene, fluorene, fluoranthene, and pyrene concentration in the skeleton and soft tissue of 7 adult and 29 old specimens of the non-zooxanthellate coral *Leptopsammia pruvoti* from the Mediterranean Sea. *Leptopsammia pruvoti* accumulated 2–72 times higher PAH concentrations than the previously investigated zooxanthellate *Balanophyllia europaea* living at the same site at shallower depth, likely in relation to the different trophic strategy. Low molecular weight PAHs were preferentially accumulated compared to high molecular weight PAHs. Detected PAHs were mainly petrogenic, consistently with local pollution sources. Populations of L. *pruvoti* immobilized PAHs in the skeleton 3–4 orders of magnitude more efficiently than *B. europaea*. This highlights the need to investigate other non-zooxanthellate species, which represent the majority of Mediterranean scleractinians, but are widely overlooked with respect to the few zooxanthellate species.

1. Introduction

Being bioconstructors, corals are extremely ecologically valuable in marine ecosystems, providing habitats for a variety of organisms, and several ecosystem services from a human health and well-being perspective. Nevertheless, they have been subjected to the most extensive and prolonged damage in recent decades (Cornwall et al., 2021; Eddy et al., 2021). Rising sea surface temperatures and ocean acidification are identified as the main environmental drivers of coral and coral reef decline worldwide (Cornwall et al., 2021). Coral disease outbreaks have also relevant implications for reef conservation and restoration (Moriarty et al., 2020). Though mitigating such global stressors remains a priority of conservation efforts, coral-reef managers seek to monitor local stressors to unravel putative synergies with global impacts (Ateweberhan et al., 2013), and to establish effective water quality thresholds to help protect ecosystem function (Nalley et al., 2021). In this regard, the impacts of chemical pollution are gaining attention as they are less understood. Much of the research effort have been addressed to inorganic chemicals, including metals and nutrients, while effects of organic pollutants with bioaccumulative and toxicity features have been poorly explored (Nalley et al., 2021).

Polycyclic aromatic hydrocarbons (PAHs; Combi et al., 2020) are the constituents of fuels and oils most harmful to the marine environment (Rocha and Palma, 2019). Natural PAH sources exist (e.g., diagenesis of organic matter, biological processes) but the main source is anthropogenic (Abdel-Shafy and Mansour, 2016; Sun et al., 2018), such as incomplete combustion of organic matter and fossil fuels (pyrogenic PAHs) or direct discharge from a variety of sources (petrogenic PAHs) (Abdel-Shafy and Mansour, 2016). Due to their physicochemical characteristics (i.e., octanol-water partition coefficient ranging from 3.2 to

* Corresponding author.
E-mail addresses: emanuela.frapiccini@cnr.it (F. Emanuela), erik.caroselli@unibo.it (C. Erik), silvia.franzellitti@unibo.it (F. Silvia), fiorella.prada2@unibo.it (P. Fiorella), mauro.marini@cnr.it (M. Mauro), s.goffredo@unibo.it (G. Stefano).
[1] Equally contributing authors.
[2] Current address: Environmental Biophysics and Molecular Ecology Program, Department of Marine and Coastal Sciences, Rutgers University, New Brunswick, NJ 08901, USA.

https://doi.org/10.1016/j.marpolbul.2022.114109
Received 16 July 2022; Received in revised form 31 August 2022; Accepted 3 September 2022
Available online 14 September 2022

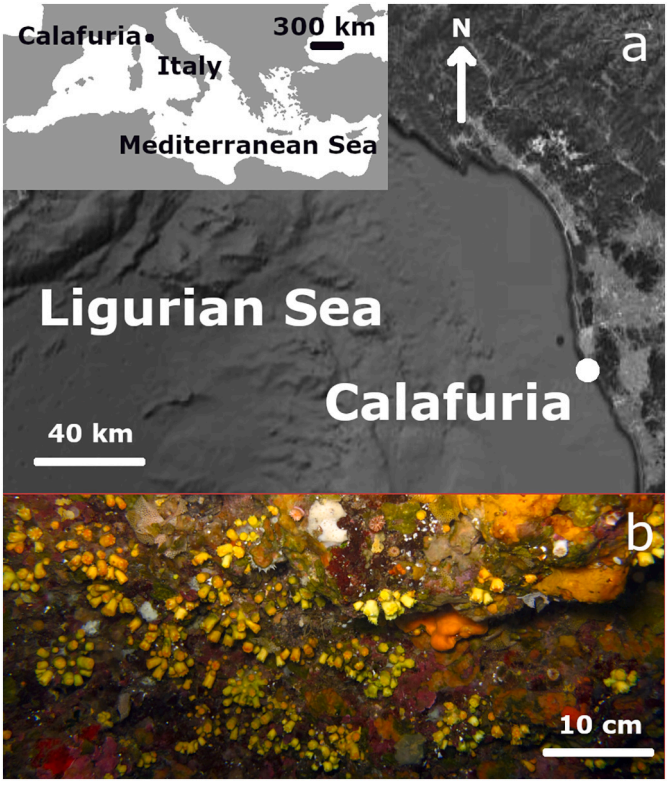

Fig. 1. Location where corals were collected. (a) Map of Calafuria (43°27′ N, 10°21′ E, Italy, Ligurian Sea). (b) Specimens of the common and abundant coral L. *pruvoti* in a crevice at 16 m in Calafuria.

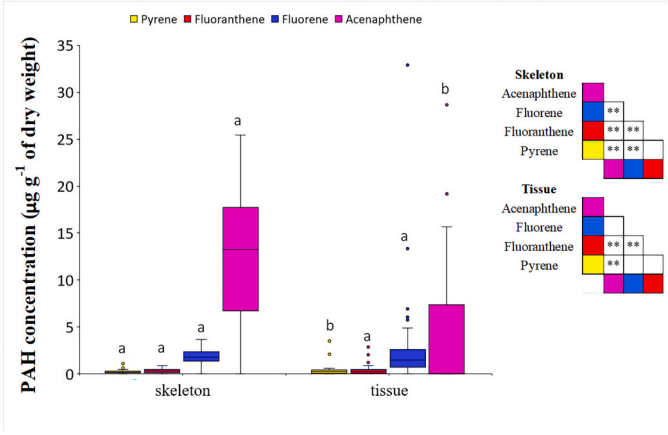

Fig. 2. Concentration (µg g^{-1} of dry weight) of PAHs in the two biological compartments of L. *pruvoti*. (a) Boxplots represent median, upper and lower quartiles ($N = 36$) of PAH concentration in coral skeleton and tissue. Different letters indicate significant differences in the concentration of each PAH between biological compartments ($P < 0.05$; PERMANOVA pairwise comparisons *t*-tests; 999 permutations). (b) Within each biological compartment, triangular matrices report differences between pairs of PAHs (**$P < 0.01$; PERMANOVA pairwise comparisons *t*-tests; 999 permutations).

5.4; Frapiccini and Marini, 2015), PAHs are easily adsorbed onto suspended particulate matter of the water column and are preferentially partitioned into sediments or biological tissues (Sun et al., 2018), making benthic organisms such as corals particularly subjected to PAH accumulation and toxicity (Caroselli et al., 2020). PAHs interfere with coral gene transcription (Woo et al., 2014), metabolism (Downs et al., 2006; Guzmán Martínez et al., 2007), tissue integrity (Guzmán Martínez et al., 2007; Renegar and Turner, 2021), larval development and settlement (Negri and Heyward, 2000; Nordborg et al., 2018). Corals can occupy multiple trophic niches thus acquiring pollutants PAHs through multiple pathways, such as direct bioconcentration from seawater or from contact with sediments, and their trophic strategies, which encompass different degree of heterotrophic nutrition (i.e. the capture of suspended particulate matter, herbivory, zooplankton predation) and autotrophy in zooxanthellate corals (i.e. the acquisition of carbon and nutrients from the photosynthetic byproducts of coral endosymbiotic zooxanthellae algae) (Ashok et al., 2022). Different factors (e.g., growth stage, lipid content, trophic strategy) play an important role on PAH accumulation in corals, but further knowledge on these interactions is needed (Li et al., 2021).

Leptopsammia pruvoti Lacaze-Duthiers, 1897 (Family: Dendrophylliidae) is a gonochoric (Goffredo et al., 2005), solitary, and non-zooxanthellate coral common on rocky bottom in the Mediterranean Sea and the NE Atlantic, reaching abundances of >10,000 individuals m^{-2} (Goffredo et al., 2010), at depths from 0 to 70 m (Zibrowius, 1980). The demography and skeletal properties of this species are well described (Caroselli et al., 2012). This study focused on acenaphthene, fluorene, fluoranthene and pyrene to allow a direct comparison with previous analyses on the zooxanthellate *Balanophyllia europaea*, which preferentially accumulated PAHs in the zooxanthellae, followed by the soft tissue, and the skeleton (Caroselli et al., 2020). As this accumulation pattern seems widespread (Ko et al., 2014; Ranjbar Jafarabadi et al., 2018), this study aimed to assess the influence of heterotrophy on PAH levels and accumulation pattern in L. *pruvoti* and confirm that skeletal storage of PAHs may be related to the coral age population structure, as previously reported for *B. europaea* (Caroselli et al., 2020), thus assessing its impact on PAH contamination in reef ecosystems. Overall, we aimed to assess coral PAH contamination in the Mediterranean Sea, a hotspot for both PAH pollution and climate change (Diffenbaugh et al., 2007; Castro-Jiménez et al., 2012), where >90 % of existing scleractinian coral species are non-zooxanthellate such as L. *pruvoti* (Zibrowius, 1980).

2. Materials and methods

2.1. Sample collection and processing

On June 12th, 2020, scuba divers haphazardly collected thirty-six L. *pruvoti* individual polyps at 16 m depth in Calafuria (Fig. 1), receiving sediments and pollutants from one of the most polluted port areas in Italy (Bertolotto et al., 2003; Iannelli et al., 2012). Upon collection, samples were transferred to the laboratory and stored at −20 °C.

The maximum oral disc length of the (*L*) of each coral was measured with Vernier calipers (Caroselli et al., 2012). The von Bertalanffy length-age relationship of this L. *pruvoti* population was applied to estimate the age of each coral (Goffredo et al., 2010), and samples were categorized either in the age class Adult (2 < age (years) ≤ 4; $N = 7$) or Old (4 < age (years) ≤ 7; $N = 29$). Coral soft tissue was separated with an airbrush methods and coral skeletons were bleached by immersion in a 10 % sodium hypochlorite (commercial bleach) solution for 3 days, dried in an oven at 50 °C for three days, and then powdered with an agate mortar (Caroselli et al., 2020). Lyophilized soft tissue and powdered skeletons were weighed with a precision balance (±0.0001 g, Scaltec) and the intra-skeletal organic matrix (OM) dry mass was assumed as 2.5 % of skeletal mass (Reggi et al., 2014). Skeletal PAH concentration of samples was normalized over OM dry mass.

2.2. PAH quantification and analysis

Acenaphthene, fluorene, fluoranthene and pyrene were extracted and purified from skeleton and soft tissue samples using Quick Easy Cheap Effective Rugged and Safe (QuEChERS) method (Table A.1). The quantification and qualification of selected PAHs were performed in

Table A.4
Results of the comparative PERMANOVA pairwise tests between biological compartments within each PAH of L. *pruvoti* (999 permutations).

Biological compartments	Acenaphthene		Fluorene		Fluoranthene		Pyrene	
	t	P	t	P	t	P	t	P
Skeleton vs tissue	3.930	**0.001**	1.034	0.312	1.852	0.067	2.217	**0.021**

t: t-Statistics; P: significance of t with Monte Carlo correction. Significant differences are indicated in bold.

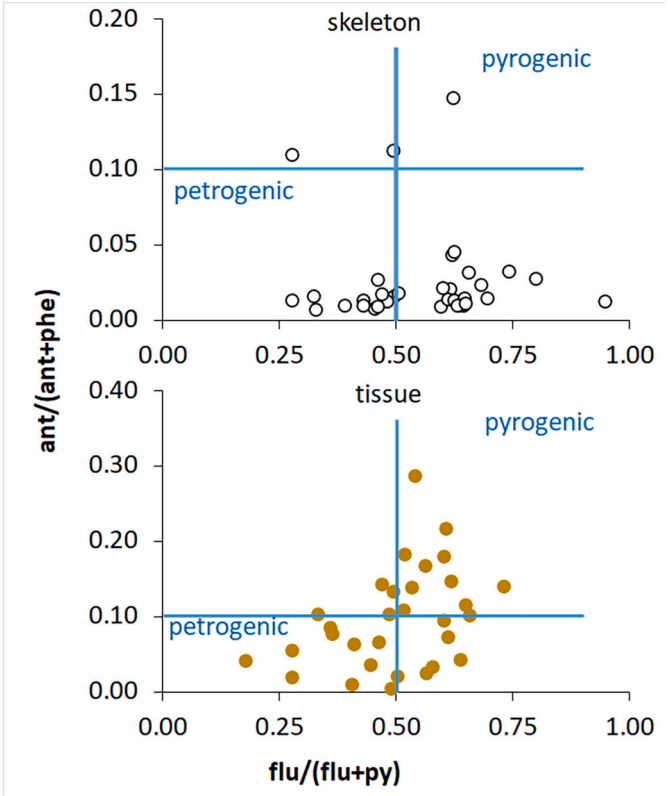

Fig. 3. Source implications of PAHs analyzed in the two biological compartments of L. *pruvoti*, using the PAH diagnostic ratios. Cross plots of the anthracene/(anthracene+phenanthrene) to fluoranthene/(fluoranthene+pyrene) ratios, the blue lines represent the petroleum/combustion transition point. (For interpretation of the references to colour in this figure legend, the reader is referred to the web version of this article.)

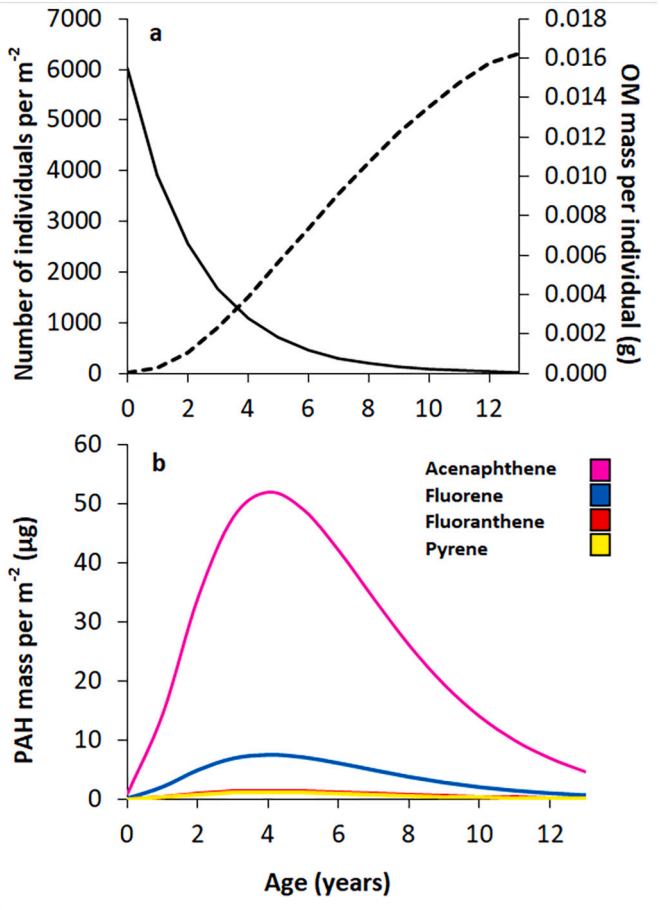

Fig. 4. PAH storage in the skeletons of L. *pruvoti* in 1 m2 of population at 16 m depth in Calafuria (Italy, Ligurian Sea), according to population age structure. (a) Distribution of the number of individuals (solid line), and OM mass (dotted line) with coral age. (b) PAH mass stored in the skeleton (blue = fluorene, pink = acenaphthene, yellow = pyrene, red = fluoranthene) over the age of L. *pruvoti* specimens. (For interpretation of the references to colour in this figure legend, the reader is referred to the web version of this article.)

UHPLC (Ultimate 3000, Thermo Scientific, Waltham, MA, USA) equipped with a fluorescence (RF2000) detector (Thermo Scientific), according to Frapiccini et al. (2020). All laboratory blanks were below the limit of quantification (LOQ). The population age structure, coral length, and skeletal mass at each age class of this L. *pruvoti* population (Goffredo et al., 2010) were used to quantify the amount of each PAH stored in 1 m^2 (for the calculation see Caroselli et al., 2020).

2.3. Statistical analyses

Concentration data were heteroskedastic and were thus compared with a permutation multivariate analysis of variance (PERMANOVA; Anderson, 2005) using Euclidean distances with software Primer 6 (Primer-e Ltd). The crossed design used three fixed factors ("PAH" with four levels: acenaphthene, fluorene, fluoranthene, pyrene; "Compartment" with 2 levels: Skeleton, Tissue; and "Age class" with 2 levels: Adult, Old), 999 permutations, and the Monte Carlo *p*-value correction due to the small sample size. A further PERMANOVA analysis with analogous settings and the factors Compartment and Age class was performed separately for each PAH.

3. Results

Acenaphthene, fluorene, fluoranthene, and pyrene concentration in the skeleton and tissue of 7 adult and 29 old individuals of L. *pruvoti* was quantified (Table 1; Table A.2). In both biological compartments, the dominant PAH was acenaphthene, followed by fluorene, fluoranthene and pyrene (Fig. 2). Fluoranthene and pyrene generally had lower concentration than fluorene and acenaphthene (Fig. 2; Tables 2; A.3). The concentration of pyrene was lower in the skeleton than in the tissue, while an opposite pattern was observed for acenaphthene (Fig. 2; Table A.4). Fluorene and fluoranthene concentrations were homogeneous in the two compartments (Fig. 2; Table A.4). These findings were also confirmed by the analysis on individual PAHs (Table 3). Age was always not significant (Tables 2, 3).

To discriminate petroleum and combustion sources of the

Table 1
Concentration (μg g^{-1} dry weight, d.w.) of the four PAHs in the biological compartments and in the two age classes of L. *pruvoti* specimens. Analogous data for *B. europaea* are added for comparison (Caroselli et al., 2020). Values are indicated as means with 95 % Confidence Intervals in parentheses. N: Number of samples.

		N	Acenaphthene (μg g^{-1} d.w.)	Fluorene (μg g^{-1} d.w.)	Fluoranthene (μg g^{-1} d.w.)	Pyrene (μg g^{-1} d.w.)
Leptopsammia pruvoti						
Skeleton	Adult	7	12 (8–17)	1.7 (1.0–2.5)	0.25 (0.11–0.39)	0.25 (0.10–0.40)
	Old	29	12 (10–15)	1.8 (1.5–2.1)	0.33 (0.25–0.41)	0.27 (0.16–0.38)
	Total	36	12 (10–15)	1.8 (1.5–2.1)	0.32 (0.25–0.39)	0.27 (0.18–0.36)
Tissue	Adult	7	3.3 (0.0–7.6)	3.1 (0.0–6.5)	0.73 (0.01–1.46)	0.86 (0.0–1.79)
	Old	29	4.1 (1.5–6.7)	3.0 (0.8–5.2)	0.33 (0.17–0.50)	0.35 (0.18–0.53)
	Total	36	4.0 (1.7–6.2)	3.0 (1.2–4.9)	0.41 (0.22–0.60)	0.45 (0.22–0.68)
Balanophyllia europaea						
Skeleton	Adult	6	0.21 (0.08–0.35)	0.24 (0.12–0.36)	0.01 (0.01–0.01)	0.04 (0.03–0.05)
	Old	7	0.13 (0.10–0.16)	0.20 (0.11–0.29)	0.01 (0.01–0.01)	0.03 (0.02–0.04)
	Total	13	0.17 (0.15–0.23)	0.22 (0.15–0.29)	0.01 (0.01–0.01)	0.04 (0.03–0.04)
Tissue	Adult	6	0.17 (0.12–0.22)	0.51 (0.34–0.69)	0.01 (0.00–0.02)	0.07 (0.03–0.12)
	Old	7	0.55 (0.05–1.04)	1.2 (0.4–2.1)	0.08 (0.05–0.10)	0.28 (0.15–0.42)
	Total	13	0.37 (0.09–0.65)	0.89 (0.41–1.37)	0.05 (0.03–0.07)	0.19 (0.09–0.28)
Zooxanthellae	Adult	6	1.1 (0.4–1.7)	2.1 (1.0–3.2)	0.09 (0.05–0.12)	0.57 (0.00–1.15)
	Old	7	0.77 (0.20–1.34)	2.1 (0.9–3.2)	0.29 (0.13–0.45)	1.0 (0.6–1.5)
	Total	13	0.91 (0.48–1.33)	2.1 (1.3–2.9)	0.20 (0.10–0.30)	0.82 (0.46–1.18)

Table 2
Results of the comparative PERMANOVA analysis for PAH concentration.

Factor	df	Pseudo-F	P
PAH	3	32.735	0.001
Compartment	1	6.9438	0.011
Age class	1	0.0013	0.975
PAH × compartment	3	13.392	0.001
PAH × age class	3	0.0707	0.973
Age class × compartment	1	0.0100	0.938
PAH × age class × compartment	3	0.0490	0.977

df: degrees of freedom; Pseudo-F: F value by permutation (Anderson et al., 2005); P: significance of pseudo-F with Monte Carlo correction.

investigated PAHs, the *anthracene/(anthracene + phenanthrene)* diagnostic ratios were plotted against the *fluoranthene/(fluoranthene + pyrene)* ones (Fig. 3; Maletić et al., 2019). PAHs in 91.2 % of skeletal samples showed *anthracene/(anthracene + phenanthrene)* values below 0.1, an indication of petroleum origin, while 2.9 % had a pyrogenic origin and 5.9 % a mixed origin, with a strong predominance of petrogenic PAHs in the skeleton (χ^2 test, $p < 0.001$; Fig. 3). In the tissue, the petrogenic origin was still dominant among samples (50.0 %), with 34.4 % having a pyrogenic component and 15.6 % a mixed origin, but in this case the difference between petrogenic and pyrogenic origin was not statistically significant (χ^2 test, $p > 0.05$; Fig. 3).

Coral skeletons in one square meter of this L. *pruvoti* population were estimated to store 355.3 μg of acenaphthene, 52.0 μg of fluorene, 9.2 μg of fluoranthene, and 7.8 μg of pyrene (Fig. 4; Table A.5).

4. Discussion

This first investigation of PAHs in a non-zooxanthellate coral species observed that *Leptopsammia pruvoti* specimens accumulated PAHs up to about 10 μg g^{-1} dry weight (d.w.) in their skeletons. The mainly petrogenic origin of detected PAHs confirms the previous study on *B. europaea* in the same area, suggesting the presence of petroleum contamination at the sampling site (Caroselli et al., 2020). A preferential accumulation of the low molecular weight PAHs fluorene and acenaphthene was observed, as in the zooxanthellate coral *B. europaea* collected at the same site at shallower depths (i.e., 6 m; Caroselli et al., 2020) and in tropical corals (Ko et al., 2014; Ranjbar Jafarabadi et al., 2018; Han et al., 2020), likely due to their higher solubility (Sverdrup et al., 2002).

PAH concentration in L. *pruvoti* was 2–72 times higher than in the analogous compartments of *B. europaea* (Table 1; Caroselli et al., 2020) and ranged similarly to Red Sea corals (0.007–0.308 vs. 0.03–0.3 μg g^{-1} over skeletal dry weight, respectively; El-Sikaily et al., 2003). Since *B. europaea* and L. *pruvoti* were collected within a few tens of meters, and within 10 m of the water column (6 m vs 16 m), their different concentration is unlikely ascribable to a different environmental burden of PAHs. A possible explanation to the observed differences between L. *pruvoti* and *B. europaea* could depend on their different energy intake strategies and therefore different trophic position and food-chain. Zooxanthellate corals like *B. europaea* can obtain most of the animal host's metabolic energy needs through translocation of photosynthate by the symbiotic algae (Muscatine, 1990), while non-zooxanthellate corals such as L. *pruvoti* feed exclusively on external particulate food sources such as phyto- and zooplankton or detrital organic matter (Ferrier-Pagès and Leal, 2019). PAHs adsorbed by particulate matter in the water column (Li et al., 2020) are uptaken by phyto- and zooplankton both directly from seawater and by feeding (Hsieh et al., 2019), with potential further transfer to low-level trophic webs (Alekseenko et al., 2018). The accumulation of the PAH phenanthrene in the tropical coral *Acropora millepora* under three treatments representing PAH exposure levels of increasing food-chain length (i.e., dissolved in seawater, exposed microalgae representing herbivory, and exposed copepods

Table 3
Results of the PERMANOVA analysis for the concentration of each of the four PAHs.

Factor	df	Acenaphthene		Fluorene		Fluoranthene		Pyrene	
		Pseudo-F	P	Pseudo-F	P	Pseudo-F	P	Pseudo-F	P
Compartment	1	15.444	0.001	1.069	0.308	3.431	0.065	4.914	0.033
Age class	1	0.053	0.818	2.73E^{-06}	0.998	1.465	0.247	2.427	0.134
Compartment × age class	1	0.024	0.877	0.004	0.948	3.409	0.065	2.824	0.090

df: degrees of freedom; Pseudo-F: F value by permutation (Anderson et al., 2005); P: significance of pseudo-F with Monte Carlo correction. Significant differences are indicated in bold.

representing predation) showed increased bioaccumulation in the treatment with PAH exposed copepods (i.e., with increased food-chain length) (Ashok et al., 2022). Thus, the increased food-chain length in L. *pruvoti* (exclusively heterotrophic) compared to *B. europaea* (mixotrophic) could partially explain the higher PAH accumulation in the former compared to the latter. The routes of initial PAH uptake of both species are likely to be the same (i.e., either feeding or through direct adsorption from the dissolved fraction). However, the balance of uptake routes is likely to differ as L. *pruvoti* relies solely on heterotrophy.

The different trophic strategies could also explain the different PAH accumulation pattern among tissue and skeleton in L. *pruvoti* and *B. europaea*. PAH accumulation pattern of all previously investigated corals from different locations is zooxanthellae > coral tissue > coral skeleton (Ko et al., 2014; Ranjbar Jafarabadi et al., 2018; Caroselli et al., 2020). Acenaphthene was the only PAH exhibiting this pattern in L. *pruvoti*. Pyrene was more concentrated in the skeleton than in the tissue, and both fluorene and fluoranthene were equally abundant in the two coral compartments. A recent model for zooxanthellate corals proposes that PAHs are transferred from zooxanthellae to the coral tissue through lipid storage, possibly following the translocation pathways of photosynthetic products from the symbiont to the host (Muscatine et al., 1981, 1984), and then to the final storage in skeleton and associated OM (Caroselli et al., 2020). Heterotrophic corals such as L. *pruvoti* or corals living at different depths (e.g., shallow vs deep) likely have different food webs and their PAH accumulation patterns may consequently differ, according to the zooplankton species involved. Different metabolic pathways, particularly those related to lipid biosynthesis and catabolism, should also be considered. Fatty acid compositions of skeletal OM is different between zooxanthellate and non-zooxanthellate corals, likely linked to the different energy intake strategies, and some are exclusively produced by either the symbiont or the host (Samorì et al., 2017). Thus, exchange of macromolecules between symbionts and the host in zooxanthellate species may determine different PAH accumulation patterns between biological compartments than in non-zooxanthellate species. Further accumulation pattern variability may derive from PAH interaction with mucus (Han et al., 2020), recirculation among biological compartments, and detoxification/biotransformation mechanisms, for which data on corals are still very scarce (Downs et al., 2012).

The long-term (13 years = maximum estimated longevity; Goffredo et al., 2010) PAH sequestration capacity of this populations of L. *pruvoti* reached a maximum in 4 years old individuals. Considering that PAHs enclosed within the calcium carbonate skeletal crystals are stored until death and further skeletal dissolution, it is important to quantify the extent of these processes under ocean acidification scenarios (IPCC, 2019). Since growth and population dynamics are characterized in L. *pruvoti* populations throughout the latitudinal extension of Italian coasts (>1000 km; Caroselli et al., 2012), the ongoing PAH assessment across this gradient may accurately evaluate coral potential to mitigate PAH pollution. It is noteworthy that the 1 m^2-normalized amount of PAH stored by L. *pruvoti* populations is 3–4 orders of magnitude higher than in *B. europaea* (Table A.5; Caroselli et al., 2020). The possible role of trophic strategies in influencing corals PAH accumulation demands further research to verify if this pattern is ubiquitous or peculiar for L. *pruvoti* and *B. europaea* (this study; Caroselli et al., 2020).

5. Conclusions

The non-zooxanthellate coral L. *pruvoti* accumulated acenaphthene, fluorene, fluoranthene and pyrene at higher concentrations than the zooxanthellate *B. europaea* (i.e., mixotrophic) living in the same site at shallower depth, likely in relation to the different trophic strategy (i.e., heterotrophy). Populations of the non-zooxanthellate L. *pruvoti* analyzed in this study immobilized PAHs in the skeleton much more efficiently than their zooxanthellate and sympatric counterpart *B. europaea*. This study highlights the need for further research efforts on: i) the overlooked non-zooxanthellate corals, as they represent the vast majority of Mediterranean scleractinian coral species (Zibrowius, 1980); ii) the different pathways by which corals accumulate PAHs; iii) the impact of different exposure modes on coral physiology; iv) PAH environmental concentrations in seawater around Mediterranean coralligenous assemblages, which are among the most threatened habitats in the Mediterranean Sea (Ingrosso et al., 2018); and v) analytically-verified biological endpoints suitable for risk assessments, urgently needed to identify local management strategies that prioritize the most important chemical contaminants of concern for marine ecosystems health. These knowledge gaps should also be addressed within the framework of future climate change scenarios and how the accumulation of these pollutants in marine organisms will interact with varying environmental conditions such as ocean warming and acidification.

CRediT authorship contribution statement

Frapiccini Emanuela: Methodology, Investigation, Writing – review & editing, Visualization. **Caroselli Erik:** Methodology, Formal analysis, Resources, Writing – review & editing, Visualization. **Franzellitti Silvia:** Methodology, Resources, Writing – review & editing. **Prada Fiorella:** Writing – review & editing. **Marini Mauro:** Conceptualization, Resources, Writing – review & editing, Supervision. **Goffredo Stefano:** Conceptualization, Resources, Writing – review & editing, Supervision.

Declaration of competing interest

The authors declare that they have no known competing financial interests or personal relationships that could have appeared to influence the work reported in this paper.

Data availability

Data will be made available on request.

Acknowledgements

The Scientific Diving School supplied technical and logistical support. The experiments comply with current Italian law.

Appendix A

Table A.1
HPLC-FLD determination of selected PAHs: slope of the calibration curve, coefficient of determination, limits of detection (LODs), limits of quantification (LOQs), and recovery (%).

PAH	Slope	Coefficient of determination (%)	LOD (ng mL^{-1})	LOQ (ng mL^{-1})	Recovery (%) (Mean ± std. dev.)
Acenaphthene	2.094	99.98	0.004	0.011	82 ± 10
Fluorene	4.106	99.95	0.002	0.005	87 ± 7
Fluoranthene	5.030	99.99	0.002	0.005	81 ± 7
Pyrene	1.717	99.93	0.004	0.013	81 ± 5

Table A.2
Length, Age and PAH concentration (μg g^{-1} dry weight, d.w.) data in the two biological compartments of each sample of L. *pruvoti*. Samples are arranged in increasing age order.

Sample code	Length (mm)	Age (yr)	Biological compartment	Acenaphthene (μg g^{-1} d.w.)	Fluorene (μg g^{-1} d.w.)	Fluoranthene (μg g^{-1} d.w.)	Pyrene (μg g^{-1} d.w.)
LPRCL50	3.45	2.8	Skeleton	20.2	3.62	0.215	0.257
			Tissue	<LOQ	0.659	0.447	0.240
LPRCL10	4.00	3.4	Skeleton	1.60	0.198	<LOQ	<LOQ
			Tissue	<LOQ	0.774	0.277	0.241
LPRCL01	4.10	3.5	Skeleton	16.8	2.29	0.329	0.199
			Tissue	3.74	1.80	0.167	0.291
LPRCL38	4.35	3.8	Skeleton	13.2	1.80	0.603	0.648
			Tissue	15.7	13.4	0.920	1.34
LPRCL12	4.40	3.9	Skeleton	9.03	1.48	0.151	0.154
			Tissue	<LOQ	1.79	2.86	3.55
LPRCL13	4.40	3.9	Skeleton	9.78	1.63	0.155	0.325
			Tissue	<LOQ	1.55	0.380	0.250
LPRCL62	4.40	3.9	Skeleton	13.5	1.15	0.289	0.177
			Tissue	3.72	1.69	0.059	0.106
LPRCL69	4.50	4.0	Skeleton	20.7	2.12	0.372	0.200
			Tissue	11.4	1.80	0.067	0.096
LPRCL17	4.60	4.1	Skeleton	8.44	1.94	0.337	0.210
			Tissue	10.9	2.86	0.084	0.436
LPRCL32	4.60	4.1	Skeleton	<LOQ	1.49	0.557	0.194
			Tissue	<LOQ	4.87	0.824	0.600
LPRCL57	4.65	4.2	Skeleton	15.7	2.43	0.711	1.11
			Tissue	0.738	<LOQ	<LOQ	<LOQ
LPRCL39	4.70	4.3	Skeleton	15.7	2.03	0.360	0.215
			Tissue	<LOQ	0.827	0.836	0.968
LPRCL05	4.75	4.3	Skeleton	<LOQ	<LOQ	<LOQ	<LOQ
			Tissue	<LOQ	1.31	0.204	0.192
LPRCL34	4.80	4.4	Skeleton	19.6	3.38	0.475	0.317
			Tissue	7.23	2.11	<LOQ	0.246
LPRCL35	4.80	4.4	Skeleton	3.94	2.05	<LOQ	<LOQ
			Tissue	<LOQ	6.06	0.820	0.630
LPRCL45	4.80	4.4	Skeleton	13.4	2.61	0.204	0.238
			Tissue	7.40	2.66	0.280	1.30
LPRCL56	4.80	4.4	Skeleton	25.4	1.36	0.371	0.203
			Tissue	<LOQ	1.02	0.259	0.274
LPRCL02	4.85	4.5	Skeleton	6.56	1.07	0.237	0.125
			Tissue	<LOQ	1.58	0.163	0.103
LPRCL67	4.90	4.6	Skeleton	24.5	2.35	0.431	0.251
			Tissue	<LOQ	0.681	0.120	0.077
LPRCL75	4.95	4.6	Skeleton	13.3	1.88	0.244	<LOQ
			Tissue	<LOQ	1.28	0.238	0.243
LPRCL14	5.00	4.7	Skeleton	25.4	2.61	0.418	0.282
			Tissue	<LOQ	2.50	0.463	0.263
LPRCL11	5.05	4.8	Skeleton	14.2	1.50	0.140	0.157
			Tissue	<LOQ	0.708	0.120	0.093
LPRCL22	5.10	4.9	Skeleton	15.9	1.81	0.612	0.267
			Tissue	<LOQ	0.423	0.245	0.207
LPRCL42	5.10	4.9	Skeleton	<LOQ	<LOQ	<LOQ	<LOQ
			Tissue	19.2	6.95	<LOQ	<LOQ
LPRCL74	5.10	4.9	Skeleton	6.14	0.820	0.100	0.117
			Tissue	<LOQ	0.712	0.235	0.086
LPRCL59	5.25	5.1	Skeleton	5.81	0.845	0.052	<LOQ
			Tissue	<LOQ	0.572	0.262	0.161
LPRCL16	5.35	5.3	Skeleton	<LOQ	2.59	0.914	0.938
			Tissue	<LOQ	<LOQ	<LOQ	<LOQ
LPRCL07	5.40	5.3	Skeleton	9.44	3.66	0.555	1.14
			Tissue	15.1	2.94	0.573	0.297
LPRCL19	5.40	5.3	Skeleton	18.1	2.27	0.517	0.285
			Tissue	7.45	0.766	<LOQ	0.087
LPRCL58	5.50	5.5	Skeleton	12.4	2.41	0.477	0.274
			Tissue	<LOQ	0.51	0.077	0.050
LPRCL04	5.95	6.4	Skeleton	7.13	0.386	0.289	0.173
			Tissue	3.04	1.20	0.037	0.074
LPRCL30	5.95	6.4	Skeleton	18.5	2.71	0.149	0.196
			Tissue	8.69	2.41	<LOQ	<LOQ
LPRCL09	6.00	6.5	Skeleton	20.3	1.75	0.353	0.468
			Tissue	<LOQ	0.517	0.142	0.160
LPRCL64	6.20	6.9	Skeleton	14.3	1.44	0.191	0.186
			Tissue	28.6	32.9	2.04	2.12
LPRCL33	6.30	7.1	Skeleton	10.7	1.56	0.309	0.196
			Tissue	<LOQ	5.73	1.21	1.19
LPRCL08	6.50	7.6	Skeleton	7.70	1.40	0.244	0.114
			Tissue	<LOQ	1.45	0.345	0.320

LOQ: limit of quantification.

Table A.3
Results of the comparative PERMANOVA pairwise tests between PAHs within each biological compartment of L. *pruvoti* (999 permutations).

PAHs	Skeleton		Tissue	
	T	P	t	P
Acenaphthene vs fluorene	6.555	**0.001**	0.352	0.729
Acenaphthene vs fluoranthene	7.549	**0.001**	2.189	**0.028**
Acenaphthene vs pyrene	7.565	**0.001**	2.134	**0.046**
Fluorene vs fluoranthene	7.483	**0.001**	2.053	**0.040**
Fluorene vs pyrene	7.494	**0.001**	1.987	0.051
Fluoranthene vs pyrene	0.394	0.664	0.399	0.651

t: t-Statistics; P: significance of t with Monte Carlo correction.
Statistically significant values are in bold ($P < 0.05$).

Table A.5
Mass of PAHs stored in the skeletons of L. *pruvoti* in 1 m^2 of the Calafuria population at 16 m depth. Data for *B. europaea* in the same site at 6 m are added for comparison (Caroselli et al., 2020). The number of age classes for the two species matches their estimated maximum individual lifespan.

Coral age (yr), t	Coral mean length (mm), L_t	Coral sk. mass (g), M_t	Coral sk. OM (mg), $M_{OM(t)}$	N of corals per m^{-2}, N_t	Cumulative OM (g m^{-2})	acenaphthene (μg m^{-2})	fluorene (μg m^{-2})	fluoranthene (μg m^{-2})	pyrene (μg m^{-2})
Leptopsammia pruvoti									
0	0.7	0.001	0.013	6004	0.1	1.0	0.2	0.03	0.02
1	2.1	0.012	0.30	3918	1.2	15	2.1	0.38	0.32
2	3.2	0.043	1.1	2557	2.8	34	5.0	0.89	0.75
3	4.1	0.093	2.3	1669	3.9	48	7.0	1.2	1.1
4	4.8	0.155	3.9	1089	4.2	52	7.6	1.4	1.1
5	5.5	0.224	5.6	711	4.0	49	7.2	1.3	1.1
6	6.0	0.295	7.4	464	3.4	42	6.2	1.1	0.92
7	6.4	0.364	9.1	303	2.7	34	5.0	0.88	0.74
8	6.8	0.429	11	198	2.1	26	3.8	0.68	0.57
9	7.1	0.488	12	129	1.6	19	2.3	0.50	0.43
10	7.4	0.542	14	84	1.1	14	2.1	0.37	0.31
11	7.6	0.589	15	55	0.8	10	1.5	0.26	0.22
12	7.7	0.630	16	36	0.6	7.0	1.0	0.18	0.15
13	7.8	0.649	16	23	0.4	4.7	0.7	0.12	0.10
			Total PAH mass			360	52	9.2	7.8
Balanophyllia europaea									
0	1.1	0.002	0.07	7.0	0.0005	0.00008	0.0001	0.000004	0.00002
1	3.2	0.036	1.0	5.3	0.0055	0.00093	0.0012	0.000046	0.00020
2	5.1	0.114	3.3	4.0	0.013	0.0023	0.0029	0.00011	0.00050
3	6.8	0.236	6.8	3.1	0.021	0.0036	0.0046	0.00018	0.00078
4	8.4	0.393	11	2.3	0.027	0.0045	0.0058	0.00022	0.00098
5	9.7	0.576	17	1.8	0.030	0.0050	0.0065	0.00025	0.0011
6	10.9	0.777	23	1.3	0.030	0.0052	0.0067	0.00026	0.0011
7	12.0	0.989	29	1.0	0.030	0.0050	0.0064	0.00025	0.0011
8	13.0	1.205	35	0.78	0.027	0.0046	0.0060	0.00023	0.0010
9	13.9	1.421	41	0.59	0.024	0.0041	0.0053	0.00020	0.0009
10	14.6	1.633	47	0.45	0.021	0.0036	0.0047	0.00018	0.0008
11	15.3	1.838	53	0.34	0.018	0.0031	0.0040	0.00015	0.0007
12	16.0	2.034	59	0.26	0.015	0.0026	0.0034	0.00013	0.0006
13	16.5	2.219	64	0.20	0.013	0.0021	0.0028	0.00011	0.0005
14	17.0	2.394	69	0.15	0.010	0.0018	0.0023	0.00009	0.0004
15	17.5	2.557	74	0.11	0.008	0.0014	0.0018	0.00007	0.0003
16	17.9	2.708	79	0.09	0.007	0.0011	0.0015	0.00006	0.0003
17	18.2	2.848	83	0.07	0.005	0.0009	0.0012	0.00005	0.0002
18	18.6	2.977	86	0.05	0.004	0.0007	0.0009	0.00004	0.0002
19	18.9	3.096	90	0.04	0.003	0.0006	0.0007	0.00003	0.0001
20	19.1	3.201	93	0.03	0.003	0.0005	0.0006	0.00002	0.0001
			Total PAH mass			0.054	0.070	0.0027	0.0012

References

Abdel-Shafy, H.I., Mansour, M.S., 2016. A review on polycyclic aromatic hydrocarbons: source, environmental impact, effect on human health and remediation. Egypt. J. Pet. 25, 107–123. https://doi.org/10.1016/j.ejpe.2015.03.011.

Alekseenko, E., Thouvenin, B., Tronczyński, J., Carlotti, F., Garreau, P., Tixier, C., Baklouti, M., 2018. Modeling of PCB trophic transfer in the Gulf of lions; 3D coupled model application. Mar. Pollut. Bull. 128, 140–155. https://doi.org/10.1016/j.marpolbul.2018.01.008.

Anderson, M.J., 2005. PERMANOVA: A FORTRAN Computer Program for Permutational Multivariate Analysis of Variance. Department of Statistics, Univ. of Auckland, New Zealand.

Ashok, A., Høj, L., Brinkman, D.L., Negri, A.P., Agusti, S., 2022. Food-chain length determines the level of phenanthrene bioaccumulation in corals. Environ. Pollut. 297, 118789 https://doi.org/10.1016/j.envpol.2022.118789.

Ateweberhan, M., Feary, D.A., Keshavmurthy, S., Chen, A., Schleyer, M.H., Sheppard, C. R.C., 2013. Climate change impacts on coral reefs: synergies with local effects, possibilities for acclimation, and management implications. Mar. Pollut. Bull. 74, 526–539. https://doi.org/10.1016/j.marpolbul.2013.06.011.

Bertolotto, R.M., Ghioni, F., Frignani, M., Alvarado-Aguilar, D., Bellucci, L.G., Cuneo, C., Picca, M.R., Gollo, E., 2003. Polycyclic aromatic hydrocarbons in surficial coastal sediments of the Ligurian Sea. Mar. Pollut. Bull. 46, 907–913. https://doi.org/10.1016/S0025-326X(03)00114-0.

Caroselli, E., Zaccanti, F., Mattioli, G., Falini, G., Levy, O., Dubinsky, Z., Goffredo, S., 2012. Growth and demography of the solitary scleractinian coral Leptopsammia pruvoti along a sea surface temperature gradient in the Mediterranean Sea. PLoS ONE 7, e37848. https://doi.org/10.1371/journal.pone.0037848.

Caroselli, E., Frapiccini, E., Franzellitti, S., Palazzo, Q., Prada, F., Betti, M., Goffredo, S., Marini, M., 2020. Accumulation of PAHs in the tissues and algal symbionts of a common Mediterranean coral: skeletal storage relates to population age structure. Sci. Total Environ. 743, 140781 https://doi.org/10.1016/j.scitotenv.2020.140781.

Castro-Jiménez, J., Berrojalbiz, N., Wollgast, J., Dachs, J., 2012. Polycyclic aromatic hydrocarbons (PAHs) in the Mediterranean Sea: atmospheric occurrence, deposition and decoupling with settling fluxes in the water column. Environ. Pollut. 166, 40–47. https://doi.org/10.1016/j.envpol.2012.03.003.

Combi, T., Pintado-Herrera, M.G., Lara-Martín, P.A., Lopes-Rocha, M., Miserocchi, S., Langone, L., Guerra, R., 2020. Historical sedimentary deposition and flux of PAHs, PCBs and DDTs in sediment cores from the western Adriatic Sea. Chemosphere 241, 125029. https://doi.org/10.1016/j.chemosphere.2019.125029.

Cornwall, C.E., Comeau, S., Kornder, N.A., Perry, C.T., van Hooidonk, R., DeCarlo, T.M., Pratchett, M.S., Anderson, K.D., Browne, N., Carpenter, R., Diaz-Pulido, G., D'Olivo, J.P., Doo, S.S., Figueiredo, J., Fortunato, S.A.V., Kennedy, E., Lantz, C.A., McCulloch, M.T., González-Rivero, M., Schoepf, V., Smithers, S.G., Lowe, R.J., 2021. Global declines in coral reef calcium carbonate production under ocean acidification and warming. Proc. Natl. Acad. Sci. U. S. A. 118, e2015265118 https://doi.org/10.1073/pnas.2015265118.

Diffenbaugh, N.S., Pal, J.S., Giorgi, F., Gao, X., 2007. Heat stress intensification in the Mediterranean climate change hotspot. Geophys. Res. Lett. 34, L11706. https://doi.org/10.1029/2007GL030000.

Downs, C.A., Richmond, R.H., Mendiola, W.J., Rougee, L., Ostrander, G.K., 2006. Cellular physiological effects of the MV kyowa violet fuel-oil spill on the hard coral, Porites lobata. Environ. Toxicol. Chem. 25, 3171–3180. https://doi.org/10.1897/05-509R1.1.

Downs, C.A., Ostrander, G.K., Rougee, L., Rongo, T., Knutson, S., Williams, D.E., Mendiola, W., Holbrook, J., Richmond, R.H., 2012. The use of cellular diagnostics for identifying sub-lethal stress in reef corals. Ecotoxicology 21, 768–782. https://doi.org/10.1007/s10646-011-0837-4.

Eddy, T.D., Lam, V.W.Y., Reygondeau, G., Cisneros-Montemayor, A.M., Greer, K., Palomares, M.L.D., Bruno, J.F., Ota, Y., Cheung, W.W.L., 2021. Global decline in capacity of coral reefs to provide ecosystem services. One Earth 4, 1278–1285. https://doi.org/10.1016/j.oneear.2021.08.016.

El-Sikaily, A., Khaled, A., El Nemr, A., Said, T.O., Abd-Alla, A.M.A., 2003. Polycyclic aromatic hydrocarbons and aliphatics in the coral reef skeleton of the Egyptian Red Sea coast. Bull. Environ. Con. Tox. 71, 1252–1259. https://doi.org/10.1007/s00128-003-8736-x.

Ferrier-Pagès, C., Leal, M.C., 2019. Stable isotopes as tracers of trophic interactions in marine mutualistic symbioses. Ecol. Evol. 9, 723–740. https://doi.org/10.1002/ece3.4712.

Frapiccini, E., Marini, M., 2015. Polycyclic aromatic hydrocarbon degradation and sorption parameters in coastal and open-sea sediment. Water Air Soil Pollut. 226, 246. https://doi.org/10.1007/s11270-015-2510-7.

Frapiccini, E., Panfili, M., Guicciardi, S., Santojanni, A., Marini, M., Truzzi, C., Annibaldi, A., 2020. Effects of biological factors and seasonality on the level of polycyclic aromatic hydrocarbons in red mullet (Mullus barbatus). Environ. Pollut. 258, 113742 https://doi.org/10.1016/j.envpol.2019.113742.

Goffredo, S., Radetić, J., Airi, V., Zaccanti, F., 2005. Sexual reproduction of the solitary sunset cup coral Leptopsammia pruvoti (Scleractinia, Dendrophylliidae) in the Mediterranean. 1. Morphological aspects of gametogenesis and ontogenesis. Mar. Biol. 147, 485–495. https://doi.org/10.1007/s00227-005-1567-z.

Goffredo, S., Caroselli, E., Mattioli, G., Zaccanti, F., 2010. Growth and population dynamic model for the non-zooxanthellate temperate solitary coral Leptopsammia pruvoti (Scleractinia, Dendrophylliidae). Mar. Biol. 157, 2603–2612. https://doi.org/10.1007/s00227-010-1522-5.

Guzmán Martínez, M.D.C., Ramírez Romero, P., Banaszak, A.T., 2007. Photoinduced toxicity of the polycyclic aromatic hydrocarbon, fluoranthene, on the coral, Porites divaricata. J. Environ. Sci. Health Part A 42, 1495–1502. https://doi.org/10.1080/10934520701480946.

Han, M., Zhang, R., Yu, K., Li, A., Wang, Y., Huang, X., 2020. Polycyclic aromatic hydrocarbons (PAHs) in corals of the South China Sea: occurrence, distribution, bioaccumulation, and considerable role of coral mucus. J. Hazard. Mater. 384, 121299 https://doi.org/10.1016/j.jhazmat.2019.121299.

Hsieh, H.-Y., Huang, K.-C., Cheng, J.-O., Lo, W.-T., Meng, P.-J., Ko, F.-C., 2019. Environmental effects on the bioaccumulation of PAHs in marine zooplankton in Gaoping coastal waters, Taiwan: concentration, distribution, profile, and sources. Mar. Pollut. Bull. 144, 68–78. https://doi.org/10.1016/j.marpolbul.2019.04.048.

Iannelli, R., Bianchi, V., Macci, C., Peruzzi, E., Chiellini, C., Petroni, G., Masciandaro, G., 2012. Assessment of pollution impact on biological activity and structure of seabed bacterial communities in the port of Livorno (Italy). Sci. Total Environ. 426, 56–64. https://doi.org/10.1016/j.scitotenv.2012.03.033.

Ingrosso, G., Abbiati, M., Badalamenti, F., Bavestrello, G., Belmonte, G., Cannas, R., Benedetti-Cecchi, L., Bertolino, M., Bevilacqua, S., Nike Bianchi, C., Bo, M., Boscari, E., Cardone, F., Cattaneo-Vietti, R., Cau, A., Cerrano, C., Chemello, R., Chimienti, G., Congiu, L., Corriero, G., Costantini, F., De Leo, F., Donnarumma, L., Falace, A., Fraschetti, S., Giangrande, A., Gravina, M.F., Guarnieri, G., Mastrototaro, F., Milazzo, M., Morri, C., Musco, L., Pezzolesi, L., Piraino, S., Prada, F., Ponti, M., Rindi, F., Russo, G.F., Sandulli, R., Villamor, A., Zane, L., Boero, F., 2018. Mediterranean bioconstructions along the Italian coast. Adv. Mar. Biol. 79, 61–136. https://doi.org/10.1016/bs.amb.2018.05.001.

IPCC, 2019. In: Pörtner, H.-O., Roberts, D.C., Masson-Delmotte, V., Zhai, P., Tignor, M., Poloczanska, E., Mintenbeck, K., Alegría, A., Nicolai, M., Okem, A., Petzold, J., Rama, B., Weyer, N.M. (Eds.), IPCC Special Report on the Ocean and Cryosphere in a Changing Climate. In press.

Ko, F.-C., Chang, C.-W., Cheng, J.-O., 2014. Comparative study of polycyclic aromatic hydrocarbons in coral tissues and the ambient sediments from Kenting National Park, Taiwan. Environ. Pollut. 185, 35–43. https://doi.org/10.1016/j.envpol.2013.10.025.

Li, H., Duan, D., Beckingham, B., Yang, Y., Ran, Y., Grathwohl, P., 2020. Impact of trophic levels on partitioning and bioaccumulation of polycyclic aromatic hydrocarbons in particulate organic matter and plankton. Mar. Pollut. Bull. 160, 111527 https://doi.org/10.1016/j.marpolbul.2020.111527.

Li, Y., Zou, X., Zou, S., Li, P., Yang, Y., Wang, J., 2021. Pollution status and trophic transfer of polycyclic aromatic hydrocarbons in coral reef ecosystems of the South China Sea. ICES J. Mar. Sci. 78, 2053–2064. https://doi.org/10.1093/icesjms/fsab081.

Maletić, S.P., Beljin, J.M., Rončević, S.D., Grgić, M.G., Dalmacija, B.D., 2019. State of the art and future challenges for polycyclic aromatic hydrocarbons is sediments: sources, fate, bioavailability and remediation techniques. J. Hazard. Mater. 365, 467–482. https://doi.org/10.1016/j.jhazmat.2018.11.020.

Moriarty, T., Leggat, W., Huggett, M.J., Ainsworth, T.D., 2020. Coral disease causes, consequences, and risk within coral restoration. Trends Microbiol. 28, 793–807. https://doi.org/10.1016/j.tim.2020.06.002.

Muscatine, L., 1990. The role of symbiotic algae in carbon and energy flux in reef corals. In: Dubinsky, Z. (Ed.), Ecosystems of the World. Coral Reefs, pp. 75–87.

Muscatine, L., McCloskey, L.R., Marian, R.E., 1981. Estimating the daily contribution of carbon from zooxanthellae to coral animal respiration. Limnol. Oceanogr. 26, 601–611. https://doi.org/10.4319/lo.1981.26.4.0601.

Muscatine, L., Falkowski, P.G., Porter, J.W., Dubinsky, Z., 1984. Fate of photosynthetic fixed carbon in light- and shade-adapted colonies of the symbiotic coral Stylophora pistillata. Proc. R. Soc. Lond. B 222, 181–202. https://doi.org/10.1098/rspb.1984.0058.

Nalley, E.M., Tuttle, L.J., Barkman, A.L., Conklin, E.E., Wulstein, D.M., Richmond, R.H., Donahue, M.J., 2021. Water quality thresholds for coastal contaminant impacts on corals: a systematic review and meta-analysis. Sci. Total Environ. 794, 148632 https://doi.org/10.1016/j.scitotenv.2021.148632.

Negri, A.P., Heyward, A.J., 2000. Inhibition of fertilization and larval metamorphosis of the coral Acropora millepora (Ehrenberg, 1834) by petroleum products. Mar. Pollut. Bull. 41, 420–427. https://doi.org/10.1016/S0025-326X(00)00139-9.

Nordborg, F.M., Flores, F., Brinkman, D.L., Agustí, S., Negri, A.P., 2018. Phototoxic effects of two common marine fuels on the settlement success of the coral Acropora tenuis. Sci. Rep. 8, 8635. https://doi.org/10.1038/s41598-018-26972-7.

Ranjbar Jafarabadi, A., Riyahi Bakhtiari, A., Aliabadian, M., Laetitia, H., Shadmehri Toosi, A., Yap, C.K., 2018. First report of bioaccumulation and bioconcentration of aliphatic hydrocarbons (AHs) and persistent organic pollutants (PAHs, PCBs and PCNs) and their effects on alcyonacea and scleractinian corals and their endosymbiotic algae from the Persian Gulf, Iran: inter and intra-species differences. Sci. Total Environ. 627, 141–157. https://doi.org/10.1016/j.scitotenv.2018.01.185.

Reggi, M., Fermani, S., Landi, V., Sparla, F., Caroselli, E., Gizzi, F., Dubinsky, Z., Levi, O., Cuif, J.P., Dauphin, Y., Goffredo, S., Falini, G., 2014. Biomineralization in Mediterranean corals: the role of the intra-skeletal organic matrix. Cryst. Growth Des. 14, 4310–4320. https://doi.org/10.1021/cg5003572.

Renegar, D.A., Turner, N.R., 2021. Species sensitivity assessment of five Atlantic scleractinian coral species to 1-methylnaphthalene. Sci. Rep. 11, 529. https://doi.org/10.1038/s41598-020-80055-0.

Rocha, A.C., Palma, C., 2019. Source identification of polycyclic aromatic hydrocarbons in soil sediments: application of different methods. Sci. Total Environ. 652, 1077–1089. https://doi.org/10.1016/j.scitotenv.2018.10.014.

Samorì, C., Caroselli, E., Prada, F., Reggi, M., Fermani, S., Dubinsky, Z., Goffredo, S., Falini, G., 2017. Ecological relevance of skeletal fatty acid concentration and composition in Mediterranean scleractinian corals. Sci. Rep. 7, 1929. https://doi.org/10.1038/s41598-017-02034-2.

Sun, R.X., Sun, Y., Li, Q.X., Zheng, X., Luo, X., Mai, B., 2018. Polycyclic aromatic hydrocarbons in sediments and marine organisms: implications of anthropogenic effects on the coastal environment. Sci. Total Environ. 640–641, 264–272. https://doi.org/10.1016/j.scitotenv.2018.05.320.

Sverdrup, L.E., Nielsen, T., Krogh, P.H., 2002. Soil ecotoxicity of polycyclic aromatic hydrocarbons in relation to soil sorption, lipophilicity and water solubility. Environ Sci Technol 36, 2429–2435. https://doi.org/10.1021/es010180s.

Woo, S., Lee, A., Denis, V., Chen, C.A., Yum, S., 2014. Transcript response of soft coral (Scleronephthya gracillimum) on exposure to polycyclic aromatic hydrocarbons. Environ. Sci. Pollut. Res. 21, 901–910. https://doi.org/10.1007/s11356-013-1958-5.

Zibrowius, H., 1980. Les scleractiniaires de la mediterraee et de l'Atlantique Nord-oriental. Mem. Inst. Oceanogr. Monaco 11, 1–284.